

RESEARCH ARTICLE



ISSN: 2321-7758

IMPROVEMENT OF POWER FLOW WITH UPFC BY USING DPC AND FUZZY LOGIC CONTROLLERS

SRINU NAIK RAMAVATH*, PRASANTH BABU NAKKA

Electrical & Electronics Department, Nalanda institute of Engineering & Technology, Sattenapalli,
Guntur Dist., A.P, INDIA

Article Received: 26/10/2014

Article Revised on: 01/11/2014

Article Accepted on:03/11/2014



SRINU NAIK RAMAVATH



PRASANTH BABU NAKKA

ABSTRACT

AC transmission lines form the backbone of the electricity grid in most countries and continents. The power flow will follow the path of least impedance and is uncontrollable, unless active grid elements are used. To enhance the functionality of the ac transmission grid, FACTS support the transmission grid with power electronics. These devices offer level of control to the transmission system operator. A transmission line equipped with a UPFC can control the balance of the transmitted power between parallel lines and as such can optimize the use of the transmission grid for all parallel power flows UPFCS are typically built with voltage-sourced converters, having a capacitor as (limited) dc energy storage a UPFC can enforce unnatural power flows in transmission grid, to maximize the power flow while maintain stability.

The Unified Power-Flow Controller (UPFC) can impose unnatural power flows in a transmission line, to maximize the power flow. Theoretically, active and reactive power flow can be controlled without overshoot & damping oscillations. This paper discusses Direct Power Control (DPC), based on instantaneous power theory, to apply the full potential of the power converter. Simulation results of a full three-phase model with non-ideal transformers, series multilevel converter, and load confirm minimal control delay, no overshoot nor damping oscillations. Shunt Converter with Fuzzy logic & Series Converter as a third-level neutral point clamped converter with DPC and simulation results comparison with other controllers. DPC & Fuzzy Controller is a valuable control technique for a UPFC.

Key Words: Direct power control, fuzzy logic controller, flexible ac transmission control (FACTS), multilevel converter, sliding mode control, unified power-flow controller (UPFC).

©KY Publications

INTRODUCTION

The electricity is considered as the backbone for industrial revolution. Today the demand and consumption of electrical energy has increased steadily. To meet this increasing demand very complex interconnected power systems are built. These complex networks are subjected to power oscillations. Power oscillations can be defined as the change in machine rotor angle around its steady state value at the natural frequency of the total electromechanical system due to disturbance. There are different types of oscillations occurring in power

system, they are: local oscillations, inter-area oscillations, inter-plant oscillations and global oscillations. Damping of these oscillations is important so as to maintain the system stability. These complex networks are subjected to power oscillations. The power flow will follow the path of least impedance and is uncontrollable, unless active grid elements are used. To enhance the functionality of the ac transmission grid, flexible ac transmission systems (FACTS) support the transmission grid with power electronic

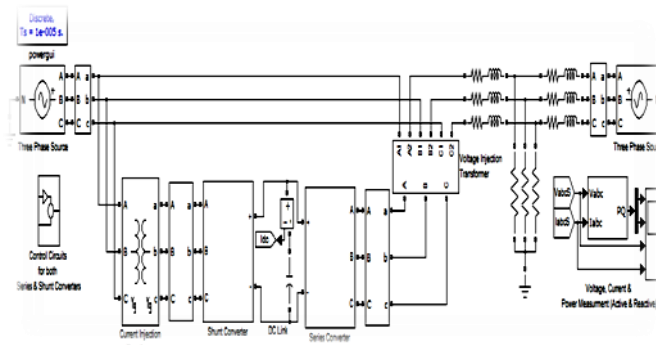


Fig. 1. Equivalent circuit of the neutral clamped VSI topology-based DSTATCOM

A unified power-flow controller (UPFC) is the most versatile of these FACTS devices. A transmission line equipped with a UPFC can control the balance of the transmitted power between parallel lines and, as such, can optimize the use of the transmission grid for all parallel power flows. A one-wire schematic of a transmission-line system equipped with a UPFC is given in Fig. 1. A UPFC is connected to the transmission line by coupling transformers, both with a shunt and with a series connection. The UPFC consists of two ac/dc converters, the ac sides connected to the shunt and series connection with the transmission line, and the dc sides connected back to back. UPFCs are typically built with voltage-sourced converters, having a capacitor as (limited) dc energy storage. In Fig. 2; an overview of the most common control structure for UPFCs is displayed. An external control describes the set points of the power system (steady state or dynamic). The internal control describes the actual power electronics and safeties of the UPFC [14][34]. The

external control is typically divided into a master and middle control [16] [34]. The master control handles targets such as an optimal power system set point, increase of transient stability, or sub synchronous resonance dampening and delivers the middle control set points. Middle control translates these master set points into set points for the series and shunt converter. The series and shunt controller can have [11][34], but do not require [10][34] and [9][34], internal communication for stability increase or optimization. The internal controller translates these middle-level control set points into switching decisions for the power-electronic components. Higher level control techniques have primarily focused on optimizing power flow [29]. Later on, the focus shifted to damping sub synchronous resonances of turbine generator shafts and inters area oscillations [3]–[8] and transient stability increase [17].[34] Various methods are used to switch intelligently.

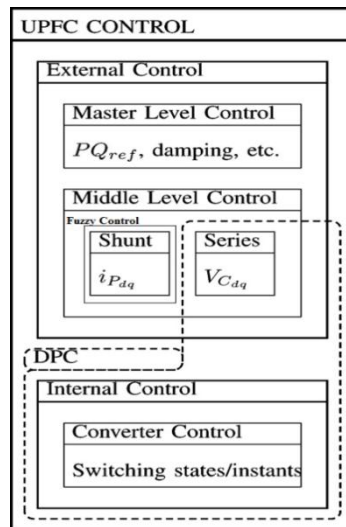


Fig. 2. UPFC controller classification according to [2] and [3], and the position of the proposed direct power controller (DPC).

Recently, a lot of interest into the increase of Grid reliability is shown [5],[34] The first designs of middle-level power-flow controllers for UPFC used direct control which suffered from serious cross coupling [27]. Decoupling control improved this cross-coupling, with high sensitivity to system parameter knowledge [15][34], and cross-coupling control of direct and quadrature series-injected voltages to active and reactive power improved on that. Cross-coupling control with direct control oscillation damping [13] enhanced performance, but based on PI control structures, realized a low control bandwidth [15],[34], [30]. The instantaneous power concept [28]-[24] enabled faster control techniques, putting, however, a larger strain on the computational capacity of the controllers [10],[34],[22]. The controller proposed in this paper combines two control levels—the middle-level series converter control and internal converter control—thereby increasing the simplicity of the controller and increasing the control dynamics. Since the series converter is typically used for power-flow control, the controller realizes a direct relation between the desired power flow and switching states, and is therefore named a direct power controller (DPC). In Fig. 2, the precise location of the proposed DPC is displayed. The direct power control technique

used in this paper finds its design principles in instantaneous power theory [23], [20],[34] and sliding mode control [18],[34],[17]. Relying on these two techniques, a sliding surface is defined in function of the instant-tenuous active and reactive power, and the system is controlled to stay on the surface. A similar controller was developed for a matrix converter [2]. This paper is a follow up paper to [19],[34], [1] with a more detailed explanation of the controller design and a comparison to other controllers.

The series and shunt converter of a UPFC are HV power electronics. To minimize the voltage stress on all components while increasing the system voltage level, multilevel neutral point clamped inverters are a promising topology. The DPC control method described in [34],[1] is divided in two parts—a general external part and an internal topology-specific part. The design principles for both are explained in detail. The external part is universal; the internal part can easily be adapted to different topologies of voltage-source converters. In this paper, a three-level neutral point clamped converter is used. Other converter topologies use the converter independent part without further theoretical development. The converter topology dependent part can be deduced analogously to the given example.

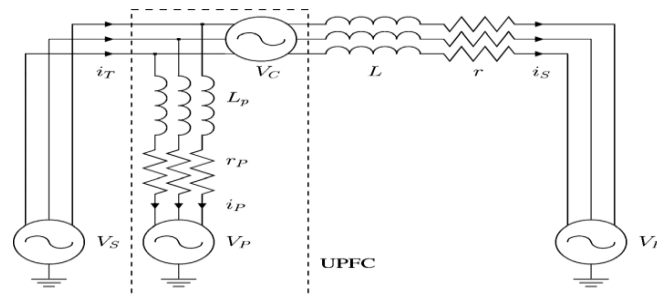


Fig. 3. Schematic of the equivalent circuit of the UPFC system.

The model of the UPFC will be developed in Section II. All assumptions made will be mentioned and clarified. In Section III, the three-level inverter's topology, its mathematical model, and the derived system equations will be explained in full. In Section IV, the direct power control will be constructed and its theoretical functionality demonstrated. The topology-dependent part is developed for a three-level NPC converter based on Section III. Simulation results are demonstrated in Section V. Conclusions regarding the DPC method and Fuzzy control, its application for UPFC, and the interaction on the control of a multilevel converter are given in Section VI.

II. UPFC SERIES CONVERTER MODEL

During model construction and controller design, power sources V_S, V_R are assumed to be infinite bus. We assume series transformer inductance and resistance negligible compared to transmission-line impedance. Connection transformers of series and shunt converters of the UPFC as in Fig. 1 are not explicitly included in the mathematical model used for controller design. Under these assumptions, we can simplify the grid as experienced by the UPFC to Fig. 3. Sending and receiving end power sources V_S, V_R are connected by transmission line. The total current drawn from the sending end i_T consists of the current flowing through the line i_S and the current exchanged with the shunt converter i_P . Shunt transformer inductance and resistance are represented by L_P and r_P . The series inductance and resistance are commonly accepted as a model for overhead transmission lines of lengths up to 80 km

[32],[34]. [1] The power to be controlled is the sending end power, formed by the current i_S and the sending end voltage V_S . This is the most realistic implementation for control purposes.

UPFC shunt converter model is similar and is not described in this paper; its functions and control are well described in literature [29], [34], [4],[1],[34] and the performance of the shunt converter is only of secondary influence on the control system described in this paper, Effects of dc bus dynamics are causes to oscillations in the real and reactive power flow which can be reduced by using fuzzy based controller. The shunt converter is only used to satisfy active power flow requirements of the dc bus.

Using the model of Fig. 3, differential equations that describe the current i_S in three phases can be formulated. Voltages $V_{abc} = V_{Sabc} + V_{Cabc} - V_{Rabc}$ are used for notation simplicity. The differential equations for the UPFC model are given as

$$\frac{d}{dt} \begin{bmatrix} i_{Sa} \\ i_{Sb} \\ i_{Sc} \end{bmatrix} = -r \begin{bmatrix} i_{Sa} \\ i_{Sb} \\ i_{Sc} \end{bmatrix} + \begin{bmatrix} V_a \\ V_b \\ V_c \end{bmatrix} \quad (1)$$

Applying the Clarke and Park transformation results in differential equations in space. Voltages $V_d = V_Sd + V_Cd - V_Rd$ and $V_q = V_Sq + V_Cq - V_Rq$ are introduced for notation simplicity. It is assumed that the pulsation ω of the grid is known and varies without discontinuities. Applying the Laplace transformation and with substitution between the two dq space transfer functions (2) is obtained,

where currents $i_{sd}(s), i_{sq}(s)$ are given in function of voltages $V_d(s)$ and $V_q(s)$.

$$\begin{bmatrix} i_{sd}(s) \\ i_{sq}(s) \end{bmatrix} = \frac{1}{L} \begin{bmatrix} (s+\frac{r}{L}) & \omega \\ \omega & (s+\frac{r}{L}) \end{bmatrix} \cdot \begin{bmatrix} V_d(s) \\ V_q(s) \end{bmatrix} \quad (2)$$

The active and reactive power of the power line is determined only by the current over the line and the sending end voltage. Without losing generality of the solution, we synchronize the Park transformation on V_{sd} , resulting in $V_{sq} = 0$ Assuming relative voltage stability. $V_{sd}(s) = V_{sd}, V_{rdq}(s) = V_{rdq}$ Active and reactive power at the sending end are calculated as

$$\begin{aligned} p_s(t) &= V_{sd} \cdot i_{sd}(t) \\ P_s(s) &= V_{sd} \cdot i_{sd}(s) \end{aligned} \quad (3)$$

$$i_{sd}(t) = -V_{sd} \cdot i_{sq}(t)$$

$$Q_s(s) = -V_{sd} \cdot i_{sq}(s)$$

Both active and reactive power consist of an uncontrollable constant part, which is determined by power source voltages v_s, v_r and line impedance L, r and a controllable dynamic part, determined by converter voltage $v_c(s)$, as made

$$\begin{aligned} P_s(s) &= P_{s0}(V_s, V_R) + \Delta P_s(V_c(s)) \\ Q_s(s) &= Q_{s0}(V_s, V_R) + \Delta(Q_s(V_c(s))) \end{aligned} \quad (4)$$

Splitting in a constant uncontrollable and a dynamic controllable part results in (5) and (6). For notation simplicity $V_{cd}(s), V_{sq}(s)$ are replaced by V_{cd}, V_{cq}

$$\begin{aligned} P_{s0}(V_s, V_R) &= V_{sd} \frac{(V_{sd} - V_{rd}) \cdot r - \omega \cdot L \cdot V_{rq}}{r^2 + (\omega \cdot L)^2} \\ Q_{s0}(V_s, V_R) &= V_{sd} \cdot \frac{(V_{rq} \cdot r + \omega \cdot L \cdot (V_{sd} - V_{rd}))}{r^2 + (\omega \cdot L)^2} \end{aligned} \quad (5)$$

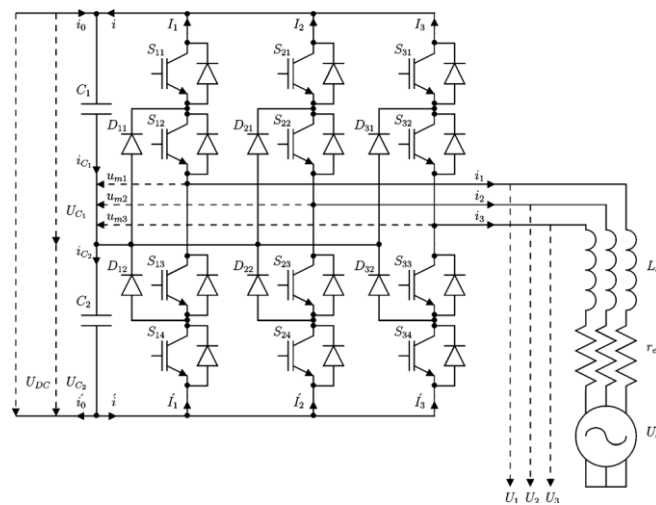


Fig. 4. Schematic of the three-level neutral point clamped converter.

$$\begin{aligned} \Delta P_s(V_c(s)) &= +V_{cd}(s) \cdot \frac{V_{sd} \cdot (L \cdot s + r)}{(L \cdot s + r)^2 + (\omega \cdot L)^2} \\ \Delta Q_s(V_c(s)) &= +V_{cd}(s) \cdot \frac{V_{sd} \cdot \omega \cdot L}{(L \cdot s + r)^2 + (\omega \cdot L)^2} - V_{cq}(s) \frac{V_{sd} \cdot (L \cdot s + r)}{(L \cdot s + r)^2 + (\omega \cdot L)^2} \end{aligned} \quad (6)$$

It is interesting to take a further look at the components of the dynamic part of the active and reactive power $\Delta p_s(s), \Delta q_s(s)$ especially at the response to steps in series converter injected voltage, $\frac{V_{cd}}{s}, \frac{V_{cq}}{s}$. Using the initial value theorem on we receive,

$$\begin{aligned} \lim_{t \rightarrow 0^+} \frac{d\Delta p_s(t)}{dt} &= \lim_{s \rightarrow \infty} s \cdot s \cdot \Delta P \left(\frac{V_c}{s} \right) = + \frac{V_{cd}}{L} \cdot V_{sd} \\ \lim_{t \rightarrow 0^+} \frac{d\Delta q_s(t)}{dt} &= \lim_{s \rightarrow \infty} s \cdot s \cdot \Delta Q \left(\frac{V_c}{s} \right) = - \frac{V_{cq}}{L} V_{sd} \end{aligned} \quad (7)$$

It is clear that only $V_{cd}(t)$ effects the derivative $\frac{d\Delta p_s(t)}{dt}$ instantaneously, and only $V_{cq}(t)$ effects the derivative $\frac{d\Delta q_s(t)}{dt}$ instantaneously.

III. THREE-LEVEL NEUTRAL POINT CLAMPED CONVERTER

The three-level neutral point clamped converter schematic is given in Fig. 4. This topology and its mathematical model have been diligently described in [21],[34]. Each leg k of the converter consists of four switching components are S_{K1} , S_{K2} , S_{K3} , S_{K4} and two diodes D_{K1} , D_{K2} and. The diodes D_{K1} , D_{K2} clamp the voltages of the connections between S_{K1} , S_{K2} and S_{K3} , S_{K4} respectively, to the neutral point, between the two capacitors C_1 , C_2 . There are three possible switching combinations for each leg k , thus three voltages u_{mk} . The system state variables are the line currents i_1 , i_2 , i_3 and the capacitor voltages, [21]. This system has the dc-bus current i_o and the equivalent load source voltages U_{EQK} as inputs. Under the assumption that the converter output voltages U_K are connected to an $r_{\epsilon q}$, $l_{\epsilon q}$ system with a sinusoidal voltage source with isolated neutral, as in Fig. 4, we can write the equations for the three-phase currents i_1 , i_2 , i_3 as in

$$L_{\epsilon q} \cdot \frac{di_k}{dt} = U_k - r_{\epsilon q} \cdot i_k - U_{\epsilon qk} \quad (8)$$

The capacitor voltages U_{C1} , U_{C2} , are influenced by the sum of the upper and lower leg currents i, i' , and the input current i_0, i'_0 as in

$$\begin{aligned} \frac{du_{c1}}{dt} &= \frac{i_{c1}}{c_1} = \frac{i_0 + i}{c_1} \\ \frac{du_{c2}}{dt} &= \frac{i_{c2}}{c_2} = \frac{i'_0 + i'}{c_2} \end{aligned} \quad (9)$$

From the restrictions on the states of the switching devices in each leg of the converter, we can define the ternary variable, representing the switching state of the entire leg, as

$$\gamma_k(t) = \begin{cases} (S_{k1}, S_{k2} = on) \wedge (S_{k3}, S_{k4} = off) \rightarrow 1 \\ (S_{k2}, S_{k3} = on) \wedge (S_{k1}, S_{k4} = off) \rightarrow 0 \\ (S_{k3}, S_{k4} = on) \wedge (S_{k1}, S_{k2} = off) \rightarrow -1 \end{cases} \quad (10)$$

To simplify this notation, combinations of this variable Γ, γ_k and Ξ are introduced.

$$\begin{aligned} \Gamma_{1k} &= \frac{\gamma_k}{2} \cdot (1 + \gamma_k) \\ \Gamma_{2k} &= \frac{\gamma_k}{2} \cdot (1 - \gamma_k) \end{aligned} \quad (11)$$

$$\begin{aligned} \Gamma_1 &= \Gamma_{11} \quad \Gamma_{12} \quad \Gamma_{13} \\ \Gamma_2 &= \Gamma_{21} \quad \Gamma_{22} \quad \Gamma_{23} \end{aligned} \quad (12)$$

$$\Xi = \frac{1}{3} \begin{bmatrix} 2\Gamma_{11} - \Gamma_{12} - \Gamma_{13} & 2\Gamma_{11} - \Gamma_{12} - \Gamma_{13} \\ -\Gamma_{11} + 2\Gamma_{12} - \Gamma_{13} & -\Gamma_{11} + 2\Gamma_{12} - \Gamma_{13} \\ -\Gamma_{11} - \Gamma_{12} + 2\Gamma_{13} & -\Gamma_{21} - \Gamma_{22} + 2\Gamma_{23} \end{bmatrix} \quad (13)$$

With this variable $\square k(t)$, and the derived variables and [21],[34], straightforward equations can be found for the description of the other variables in the system. Combining the equations of the system dynamics (14) and (7), the complete system equation is (5) [21], where $\Xi(\square 123)$, $\Gamma_1(\square 123)$, $\Gamma_2(\square 123)$, are aiding functions describing the precise dynamics in function of the switching state. It is important to realize that this system equation is not constant, nor continuous

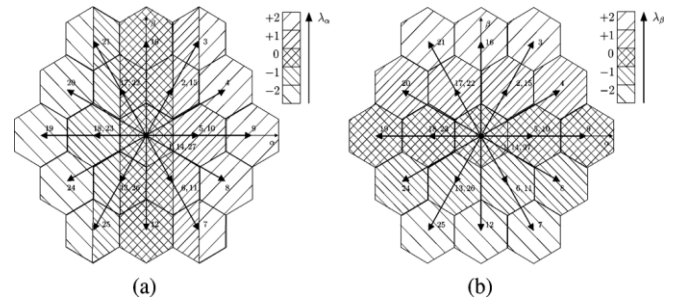


Fig. 5. Vector arrangement in five levels in α, β , for three-level three-phase converter. (a) Five levels in α , (b) Five levels in β . If we assume the voltage balance of the capacitors C_1, C_2 the 27 possible combinations of leg switching state variables $\gamma_1, \gamma_2, \gamma_3$ lead to 27 sets of phase voltages U_1, U_2, U_3 and 27 voltage vectors after Clark transformation to space. The 27 voltage vectors can be divided in 24 active vectors and 3 null vectors. The 24 active vectors form 18 unique vectors; 12 vectors form 6 redundant pairs. The 3 null vectors also form only 1 unique vector. This results in 19 different voltage vectors. To simplify the vector

selection, the 27 vectors are grouped into 5 levels in the and dimension, based on their component in this dimension. The levels and vector grouping are represented in Fig. 5. Each combination of levels corresponds to one unique voltage vector. Assuming that the capacitors C_1, C_2 and have equal capacity and using the relation of the three line currents $i_1 + i_2 + i_3 = 0$, the dynamics of the voltage balance $U_{c1} - U_{c2}$ can be derived from (5), leading to In Table I, the effect of the output voltage vectors on the capacitor voltage balance is listed.

$$\frac{d(U_{c1} - U_{c2})}{dt} = \frac{\gamma_3^2 - \gamma_2^2}{c} i_1 + \frac{\gamma_3^2 - \gamma_1^2}{c} i_2 \quad (14)$$

Comparing these values with those of $\gamma_{123} i_{123}$ for the values of the redundant vectors, given in bold,

they depend on the same currents and except for the sign, are equal. To know the sign of the derivative of the voltage unbalance $U_{c1} \cdot U_{c2}$, the sign of the instantaneous active power will be used. Since U_{dc} will always be positive, the sign of depends only on the sign of. Assuming perfect voltage balance, the instantaneous outgoing power of the converter is given by the internal product of the switching state variables and outgoing line currents scaled by the capacitor voltage by

$$P = \gamma_{123} \cdot i_{123} \cdot \frac{U_{dc}}{2} \quad (15)$$

TABLE I
 OUTPUT VOLTAGE VECTORS

Vector	γ_1	γ_2	γ_3	$C \cdot d(U_{C1} - U_{C2}) / dt$	$\gamma_{123} \cdot i_{123}$
1	1	1	1	0	0
2	1	1	0	$-i_1 - i_2$	$i_1 + i_2$
3	1	1	-1	0	$2 \cdot (i_1 + i_2)$
4	1	0	-1	i_2	$2 \cdot i_1 + i_2$
5	1	0	0	$-i_1$	i_1
6	1	0	1	i_2	$-i_2$
7	1	-1	1	0	$-2 \cdot i_2$
8	1	-1	0	$-i_1 - i_2$	$i_1 - i_2$
9	1	-1	-1	0	$2 \cdot i_1$
10	0	-1	-1	i_1	i_1
11	0	-1	0	$-i_2$	$-i_2$
12	0	-1	1	i_1	$-i_1 - 2 \cdot i_2$
13	0	0	1	$i_1 + i_2$	$-i_1 - i_2$
14	0	0	0	0	0
15	0	0	-1	$i_1 + i_2$	$i_1 + i_2$
16	0	1	-1	i_1	$i_1 + 2 \cdot i_2$
17	0	1	0	$-i_2$	i_2
18	0	1	1	i_1	$-i_1$
19	-1	1	1	0	$-2 \cdot i_1$
20	-1	1	0	$-i_1 - i_2$	$-i_1 + i_2$
21	-1	1	-1	0	$2 \cdot i_2$
22	-1	0	-1	i_2	i_2
23	-1	0	0	$-i_1$	$-i_1$
24	-1	0	1	i_2	$-2 \cdot i_1 - i_2$
25	-1	-1	1	0	$-2 \cdot (i_1 + i_2)$
26	-1	-1	0	$-i_1 - i_2$	$-i_1 - i_2$
27	-1	-1	-1	0	0

IV. DIRECT POWER CONTROL

Direct power control must ensure that the sending end power $p_S(t), q_S(t)$ follows power references $p_{Sref}(t), q_{Sref}(t)$. Defining the strong relative degree [17] of the controlled output $p_S(t), q_S(t)$, as the minimum i th-order time

derivative $\frac{d^i(p_S(t))}{dt^i}, \frac{d^i(q_S(t))}{dt^i}$ that contains a nonzero explicit function of the control vector V_C , a suitable sliding surface is a linear combination of the phase canonical state variable errors. For $p_S(t), q_S(t)$ and, $i=1$, then

$$\begin{aligned}
 s_d(t) &= k. (p_{sref}(t) - p_s(t)) = 0 \\
 s_q(t) &= k. (q_{sref}(t) - q_s(t)) = 0 \\
 \dot{s}_d(t) &= k. (\Delta p_{sref}(t) - \Delta p_s(t)) = 0 \\
 \dot{s}_q(t) &= k. (\Delta q_{sref}(t) - \Delta q_s(t)) = 0
 \end{aligned}
 \tag{16}$$

In above equation k is a strictly positive constant; therefore, the only possibility for the system to uphold the surface equations $s_d(t), s_q(t) = 0$, is having the real power $p_s(t), q_s(t)$, follow the references $p_{sref}(t), q_{sref}(t)$. A control law that enforces the system to stay on these surfaces, or move toward them at all times, can be expressed as in (28), [18], [31]

$$\begin{aligned}
 S_d(t).s_d(t) &< 0 \\
 S_q(t).s_q(t) &< 0
 \end{aligned}
 \tag{17}$$

Where $S_d(s), S_q(s)$ are governed by system dynamics involved (6). To uphold (18), the inverter has to appropriately change the sign of the derivatives $\dot{s}_d(t), \dot{s}_q(t)$. Using the results of the initial value theorem on the derivative of the sending end power in (7), the following equation can be developed

$$\begin{aligned}
 \lim_{t \rightarrow 0^+} \frac{ds_d(t)}{dt} &= \lim_{s \rightarrow \infty} s.s.S_d(s) \\
 \lim_{t \rightarrow 0^+} \frac{ds_q(t)}{dt} &= \lim_{s \rightarrow \infty} s.s.S_q(s) \\
 \lim_{t \rightarrow 0^+} \frac{ds_d(t)}{dt} &= \lim_{s \rightarrow \infty} K.s.s. (\Delta P_{sref}(s)) - k \frac{v_{cd}v_{sd}}{L} \\
 \lim_{t \rightarrow 0^+} \frac{ds_q(t)}{dt} &= \\
 \lim_{s \rightarrow \infty} K.s.s. (\Delta Q_{sref}(s)) &+ k \frac{v_{cq}v_{sd}}{L}
 \end{aligned}
 \tag{18}$$

From above equation it can be concluded that to instantaneously influence $s_d(t), V_{cd}(t)$, should be used. Similarly $s_q(t)$, for, it is done best by $V_{cd}(t)$. It is also clear from above equation that impulse or step changes in $\Delta p_{sref}(t), \Delta q_{sref}(t)$, cannot be followed instantaneously, yet ramps in, can be followed, providing their rate of change is less than

$$\begin{aligned}
 (\max(v_{cd})/L).v_{sd}, (\max(v_{cq})/L) \text{ and the} \\
 \text{combination cannot exceed} \\
 \frac{d\Delta q_{sref}(t^2)}{dt} + \frac{d\Delta p_{sref}(t^2)}{dt} < \frac{V_{cmax}^2.V_{sd}^2}{L^2}
 \end{aligned}
 \tag{19}$$

Considering this conclusion, it is important to determine the conditions to reach the direct power control surfaces using the final value theorem

$$\begin{aligned}
 \lim_{t \rightarrow \infty} S_d(t) &= \lim_{s \rightarrow 0} s.S_d(s) \\
 \lim_{t \rightarrow \infty} S_q(t) &= \lim_{s \rightarrow 0} s.S_q(s) \\
 \lim_{t \rightarrow \infty} S_d(t) &= \lim_{s \rightarrow 0} K.s. (\Delta P_{sref}(s)) - \\
 &k \frac{v_{sd}}{r^2 + \omega^2.L^2} \\
 &(V_{cd}.r + V_{cq}.\omega.L) \\
 \lim_{t \rightarrow \infty} S_q(t) &= \lim_{s \rightarrow 0} K.s. (\Delta Q_{sref}(s)) + \\
 &k \frac{v_{sd}}{r^2 + \omega^2.L^2} (V_{cd}.\omega.L - V_{cq}.r)
 \end{aligned}
 \tag{20}$$

From using the above equation several important conclusions can be drawn. The control can only handle limited steps or ramps of decaying derivative in references. Also, a clear limit exists to the controllable reference steps, limited by the maximum UPFC series output voltage amplitude,

$$\Delta P_{sref}(t^2) + \Delta q_{sref}(t^2) < V_{sd}^2 \cdot \frac{V_{cmax}^2}{r^2 + \omega^2.L^2}
 \tag{21}$$

To select a physical voltage vector, this decision process is transformed to the domain, remaining with requested changes of the UPFC series output voltage in to the output voltage vector. To limit the switching frequency, the decision is suppressed until the system state crosses a parallel surface at a certain distance from the direct power control surfaces ΔS . Note that this requested change is not expressed in a numeric value of the requested change, but as the direction of change (in this case, a ternary variable, indicating increase, no change 0, decrease -1). Depending on the currently used output vector and the requested change in, an appropriate next vector can be selected. This concludes the converter topology independent part of the controller. In Fig. 6, in the selection Desired change in to output Voltage, for a three-level NPC converter, the voltage vector selection is displayed. DPC

demands increasing or decreasing the output voltage vector in the and direction.

Based on the currently applied vector and this demand, the next vector is selected. This is simplified to selection of the voltage vector levels.

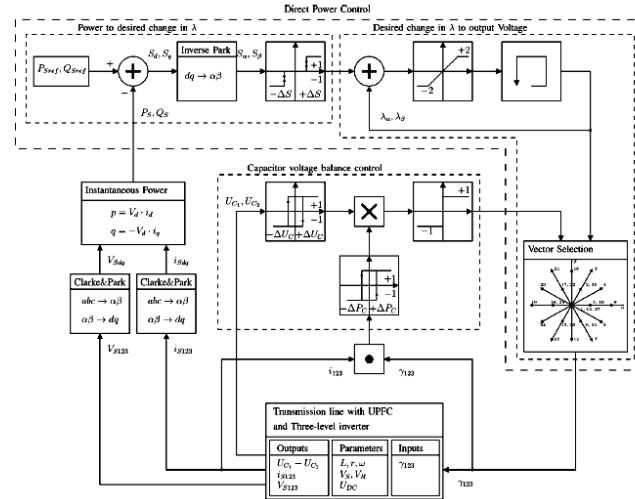


Fig. 6. Overview of the control algorithm.

TABLE II
 VECTOR ARRANGEMENT IN FIVE LEVELS
 IN α, β . (a) $U_{c1} - U_{c2} \cdot P > 0$. (b) $U_{c1} - U_{c2} \cdot P < 0$

$\frac{\lambda_{\alpha}}{\lambda_{\beta}}$	(a)					(b)					
	-2	-1	0	1	2	-2	-1	0	1	2	
2	21	21	16	3	3	2	21	21	16	3	3
1	20	17	2,17	2	4	1	20	22	15,22	15	4
0	19	18	1,14,27	5	9	0	19	23	1,14,27	10	9
-1	24	13	6,13	6	8	-1	24	26	11,26	11	8
-2	25	25	12	7	7	-2	25	25	12	7	7

In the cases that vectors coincide, an extra criterion is needed to unambiguously select a set of switching state variables, $\gamma_1, \gamma_2, \gamma_3$. Even though the voltage vectors U_1, U_2, U_3 may realize the same phase voltages, the precise switching state, also determines whether energy is drawn from or into two capacitors U_{c1} and U_{c2} .

$$(U_{c1} - U_{c2}) \cdot \frac{d(U_{c1} - U_{c2})}{dt} < 0 \quad (22)$$

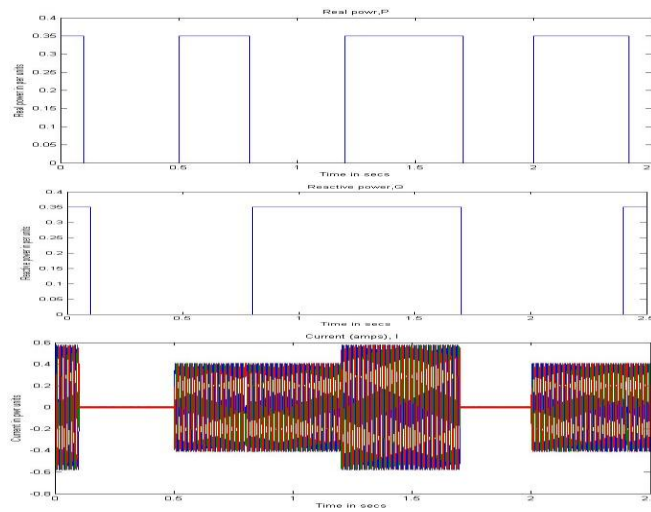
Maintain voltage balance $(U_{c1} - U_{c2})=0$, From above equation (22) must be upheld at all times. This is displayed in Fig. 6 in selection Capacitor voltage balance control. Depending on the sign of the voltage unbalance $(U_{c1} - U_{c2})$ and output power, the voltage vector can be selected so that (22) is upheld. Vector selection, in function of demand for change of the voltage vector in ,

dimension and capacitor voltage unbalance is given in Table II(a) and (b). To limit the output frequency, the size of the voltage unbalance $(U_{c1} - U_{c2})$ has to reach a certain level ΔU_c before it is addressed. In this application, it is enforced by a relay system. The last degree of freedom is within the selection of the null vector 1, 14, 27. They have the same effect on the output voltage U and capacitor voltage imbalance $U_{c1} - U_{c2}$. To minimize the switching losses, the null vector could be chosen within least switching distance from the previous vector. As such, any order from a higher controller to change the output voltage U in $\alpha\beta$ is translated unambiguously into a voltage-output vector. This voltage vector selection Method is well covered, including the necessary balancing of the capacitor voltages by [32],[34].

V. SIMULATION RESULTS& TABLES

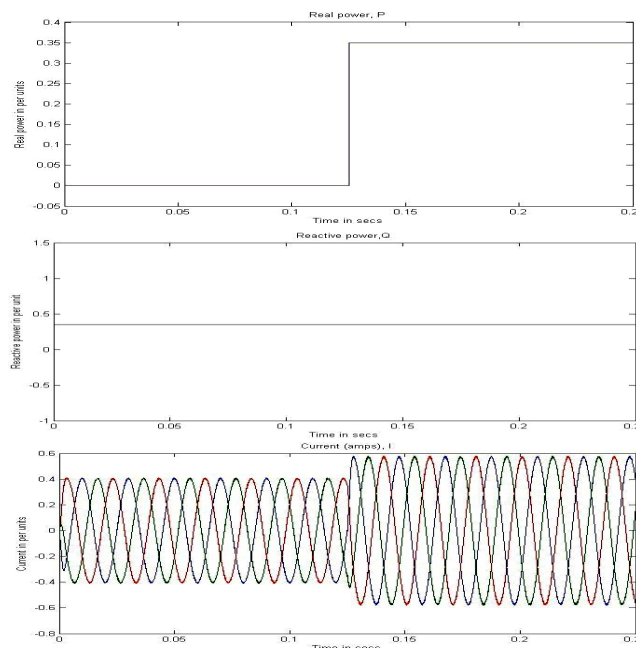
The discussed controller is demonstrated in simulation and in experimental results. Fig. 7 shows the experimental setup. A Space controller board is used. For controlled startup and ease of use, an autotransformer is used to regulate the mains voltage on the setup. Two isolation transformers are connected to the autotransformer, to represent the sending and receiving end voltages V_S, V_R . Iron

cored coils are used to represent the load impedance L_0, r_0 and transmission-line impedances L_1, r_1 , and L_2, r_2 . Another step down isolation transformer is used for the series connection of the UPFC inverter to the grid. Both the simulation and experimental setups use these parameter values so that results can be compared.



(a)

Fig 8:UPFC series converter controlling power flow under balanced conditions, 2.5-s view during stepwise changes of active and reactive power flow reference P_{ref}, Q_{ref} , . (a) Simulation (P 948 Wpu, Q 948 VARpu) (i_a, i_b, i_c , , 2.38 Apu).



(b) Fig.8:UPFC series converter controlling the power flow under balanced conditions, 250-ms view during stepwise change of active and reactive power flow reference P_{ref}, Q_{ref} Simulation (P 948Wpu, Q948 VARpu)

$(U_{3a}, U_{3b}, U_{3c}, 230 \text{ Vpu}) (i_a, i_b, i_c, 2.38 \text{ Apu}).$

Specifications

Name	Value	Unit	p.u. Value
V_b	230.0	V	1.0
S_b	948.0	VA	1.0
I_b	2.38	A	1.0
Z_b	55.8	Ω	1.0
L_1	15.0	mH	0.0845
r_1	0.1	Ω	0.002
L_2	12.0	mH	0.0675
r_2	0.1	Ω	0.002
r_0	300.0	Ω	5.38
L_m	15.0	mH	0.0845
U_{DC}	150.0	V	0.6522
ΔS	0.125	VA	0.000132
$\Delta(U_{DC})$	2.0	V	0.0087
Switching freq.	2KHz		
Length of the line	80Km		

The simulation is based on a full three-phase model of the UPFC and the power lines constructed with Mat lab Simulink. It contains a model of the converter based on the dynamic equations and control laws as described in Section IV. UPFC shunt converter and dc capacitor dynamics are included in the system model. The shunt converter is set to control the total dc voltage level of the converter dc bus the problems associated with the other PI controller can be eliminated by the Fuzzy logic control. No reactive power transfer between the shunt converter and the sending end bus is set; the sending and receiving end are simulated as infinite bus. The transformers are modeled as saturable transformers. In the first set of results, the DPC method is put to demonstrate power-flow control.

A. DPC Simulation in Balanced Conditions

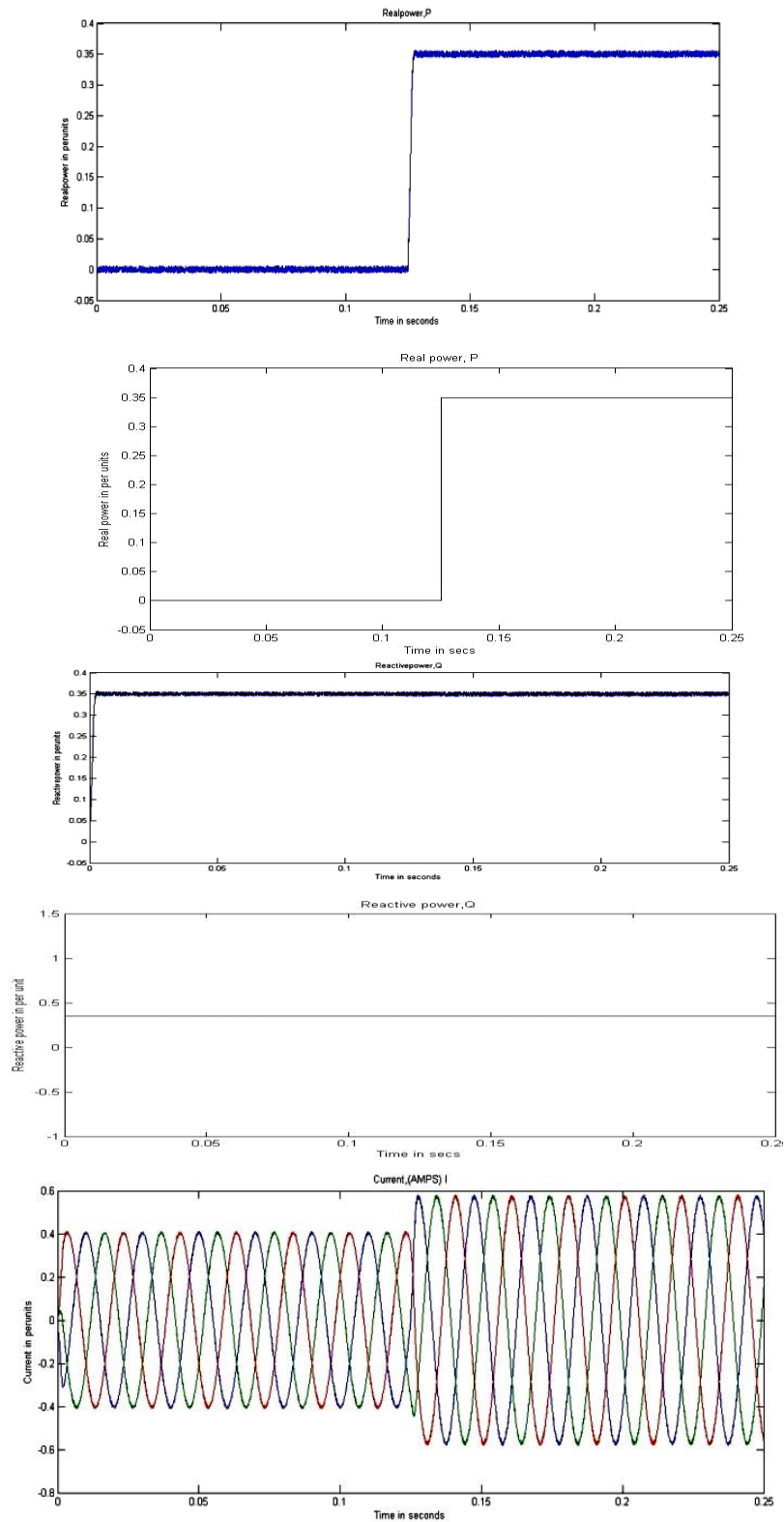
In simulation the values of 0 to 0.316 p.u. and change stepwise. It should be noted that the references, do not represent a realistic reference profile. An overview of 2.5 s of the closed-loop controlled output in Fig. 8(a) demonstrates that the system can handle any combination of sending end power references P_{Sref}, Q_{Sref} , and reference

changes $\Delta p_{Sref}, \Delta q_{Sref}$. A more detailed look at the results in Fig. 8(b) shows that there are no low-frequency phenomena in the currents, and that they are balanced. The direct power controlled system demonstrates no overshoot, no cross coupling, no steady-state, and a fast rising and settling time.

B. Comparison of wave forms of Fuzzy controller with other controllers on Shunt Converter

The same simulation model is used as in the previous test. The DPC will be compared with two other controllers: advanced dynamic control (ADC) [10] and dynamic inverse control (DIC) [22]. Both are middle-level controllers, with a clearly described design methodology. The controllers are designed as specified in their sources. To create fair comparison conditions, the converter control is implemented by a sliding mode controller for the three level converters with the same switching frequency, switching table, and relay widths as the one incorporated in the DPC [21],[34]. The comparison in this paper is given for Fuzzy controller and the PI controller obtained in [1] of the Shunt converter for better power flow of Transmission line. By this fuzzy controller the Capacitor Voltage is maintained

constant during switching operations of the converters.



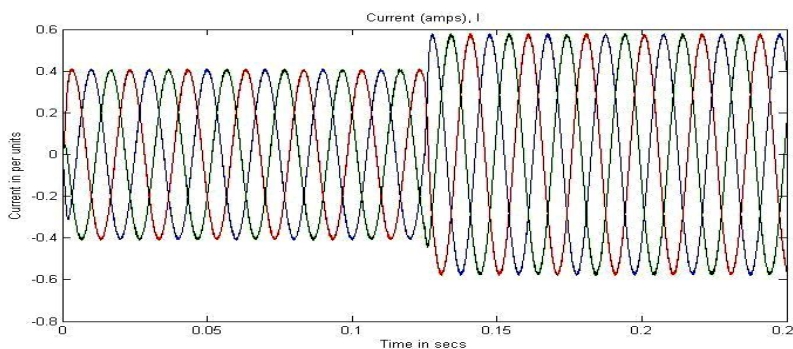


Fig8(c) UPFC series converter controlling real and reactive power flow, comparison between controllers Fuzzy and PI of Shunt converter with DPC controller on series converter under step wise changes.

CONCLUSION

The DPC technique was applied on a series converter of UPFC to control the power flow on a transmission line. The technique has been described in detail and applied to a three-level NPC converter. The main benefits of the control technique are fast dynamic control behavior with no cross coupling or overshoot, with a simple controller, independent of nodal voltage changes. The realization was demonstrated by simulation results on a scaled model of a transmission line. The Fuzzy controller was applied on shunt converter for better power flow in transmission line and the controller was compared to other PI controllers under balanced and unbalanced conditions, and demonstrated better performance, with shorter settling times, no overshoot, and in difference to voltage unbalance. We conclude that direct power control and Fuzzy controller is an effective method that can be used with UPFC. It is readily adaptable to other converter types than the three-level converter demonstrated in this paper.

REFERENCES

- [1] Jan Verweken, Fernando Silva, Dionísio Barros and Johan Driesen, "Direct Power Control of Series Converter of Unified Power-Flow Controller With Three-Level Neutral Point Clamped Converter", IEEE Trans. Power Delivery, vol. 27, no. 4, pp.1772-1782 oct.2012.
- [2] J. Monteiro, J. Silva, S. Pinto, and J. Palma, "Matrix converter-based unified power-flow controllers: Advanced direct power control method," IEEE Trans. Power Del., vol. 26, no. 1, pp. 420–430, Jan.2011.
- [3] S. Jiang, A. Gole, U. Annakkage, and D. Jacobson, "Damping performance analysis of ipfc and upfc controllers using validated small-signal Models," IEEE Trans. Power Del., vol. 26, no. 1, pp. 446–454, Jan. 2011.
- [4] X. Jiang, J. Chow, A.-A. Edris, B. Fardanesh, and E. Uzunovic, "Transfer path stability enhancement by voltage-sourced converter- based facts controllers," IEEE Trans. Power Del., vol. 25, no.2, pp. 1019–1025, Apr. 2010.
- [5] A. Rajabi-Ghahnavieh, M. Fotuhi-Firuzabad, M. Shahidehpour, and R. Feuillet, "Upfc for enhancing power system reliability," IEEE Trans. Power Del., vol. 25, no. 4, pp. 2881–2890, Oct. 2010.
- [6] M. Zarghami, M. Crow, J. Sarangapani, Y. Liu, and Scarcity, "A novel approach to interarea oscillation damping by unified power flow controllers utilizing ultra capacitors," IEEE Trans. Power Syst., vol. 25, no. 1, pp. 404–412, Feb. 2010.
- [7] J. Guo, M. Crow, and J. Sarangapani, "An improved upfc control for oscillation damping," IEEE Trans. Power Syst., vol. 24, no. 1, pp. 288–296, Feb. 2009.
- [8] S. Ray and G. Venayagamoorthy, "Wide-area signal-based optimalneurocontroller for a upfc," IEEE Trans. Power Del., vol. 23, no. 3, pp. 1597–1605, Jul. 2008.
- [9] L. Liu, P. Zhu, Y. Kang, and J. Chen, "Power-flow control performance analysis of a unified power-flow controller in a novel control scheme," IEEE Trans. Power Del., vol. 22, no. 3, pp. 1613–1619, Jul. 2007.

- [10] H. Fujita, H. Akagi, and Y. Watanabe, "Dynamic control and performance of a unified power flow controller for stabilizing a transmission system," *IEEE Trans. Power Electron.*, vol. 21, no. 4, pp. 1013–1020, Jul. 2006.
- [11] H. Wang, M. Jazaeri, and Y. Cao, "Operating modes and control interaction analysis of unified power flow controllers," *Proc. Inst. Elect. Eng., Gen., Transm. Distrib.* vol. 152, no. 2, pp. 264–270, Mar. 2005.
- [12] Z. Huang, Y. Ni, C. Shen, F. Wu, S. Chen, and B. Zhang, "Application of unified power flow controller in interconnected power systems-modeling, interface, control strategy, and case study," *IEEE Trans. Power Syst.*, vol. 15, no. 2, pp. 817–824, May 2000.
- [13] H. Fujita, Y. Watanabe, and H. Akagi, "Control and analysis of a unified power flow controller," *IEEE Trans. Power Electron.*, vol. 14, no. 6, pp. 1021–1027, Nov. 1999.
- [14] X. Lombard and P. Therond, "Control of unified power flow controller: Comparison of methods on the basis of a detailed numerical model," *IEEE Trans. Power Syst.*, vol. 12, no. 2, pp. 824–830, May 1997.
- [15] I. Papic, P. Zunko, D. Povh, and M. Weinhold, "Basic control of unified power flow controller," *IEEE Trans. Power Syst.*, vol. 12, no. 4, pp. 1734–1739, Nov. 1997.
- [16] L. Gyugyi, C. Schauder, S. Williams, T. Rietman, D. Torgerson, and A. Edris, "The unified power flow controller: A new approach to power transmission control," *IEEE Trans. Power Del.*, vol. 10, no. 2, pp. 1085–1097, Apr. 1995.
- [17] J. Hung, W. Gao, and J. Hung, "Variable structure control: A survey," *IEEE Trans. Ind. Electron.*, vol. 40, no. 1, pp. 2–22, Feb. 1993.
- [18] V. I. Utkin, "Variable structure systems with sliding modes," *IEEE Trans. Autom. Control*, vol. AC-22, no. 2, pp. 212–222, Apr. 1977.
- [19] J. Verveckken, F. A. Silva, D. Barros, and J. Driesen, "Direct power control for universal power flow controller series converter," in *Proc. IEEE ECCE Conf.*, 2010, pp. 4062–4067.
- [20] S. Venkateschwarlu, B. P. Muni, A. D. Rajkumar, and J. Praveen, "Direct power control strategies for multilevel inverter based custom power devices," *Int. J. Elect. Syst. Sci. Eng.*, vol. 1, no. 2, pp. 94–102, 2008.
- [21] F. A. Silva and S. F. Pinto, "Control methods for switching power converters," in *Power Electronics Handbook*, M. H. Rashid, Ed., 2nd. London, U.K.: Academic/Elsevier, 2007, pp. 935–998.
- [22] J. Verveckken, F. Silva, and J. Driesen, "Design of inverse controller with cross-coupling suppression for UPFC series converter," in *Proc. EUROCON Int. Conf. Comp. Tool*, Warsaw, Poland, Sep. 9–12, 2007, pp. 2613–2619.
- [23] M. K. P. Antoniewicz, "Predictive direct power control of three phase boost rectifier," *Bull. Polisch Acad. Sci.*, vol. 54, no. 3, 2006.
- [24] C. Yam, and M. Haque, "A svd based controller of upfc for power flow control," *Elect. Power Syst. Res.*, no. 70, pp. 79–84, 2004.
- [25] K. Sedraoui, K. Al-haddad, A. Chandra, and G. Olivier, "Versatile control strategy of the unified power flow controller," *Proc. Can. Conf. Elect. Comput. Eng.*, vol. 1, pp. 142–147, 2000.
- [26] S. Limyingcharoen, U. Annakkage, and N. Pahalawaththa, "Effects of unified power flow controllers on transient stability," *Proc. Inst. Elect. Eng., Gen., Transm. Distrib.* vol. 145, no. 2, pp. 182–188, Mar. 1998.
- [27] K. Smith, L. Ran, and J. Penman, "Dynamic modeling of a unified power flow controller," *Proc. Inst. Elect. Eng., Gen., Transm. Distrib.* vol. 144, no. 1, pp. 7–12, Jan. 1997.
- [28] H. Kim and H. Akagi, "The instantaneous power theory based on mapping matrices

- in three-phase four-wire systems,” in Proc. Power Convers.Conf., 1997, pp. 361–366.
- [29] L. Gyugyi, “Unified power-flow control concept for flexible ac transmission systems,” Proc. Inst. Elect. Eng., Gen., Transm. Distrib, vol.139, no. 4, pp. 323–331, Jul. 1992.
- [30] S. D. Round, Q. Yu, L. E. Norum, and T. M. Undeland, “Performance of a unified power flow controller using a d-q control system,” in Proc. 6th Int. AC and DC Power Transmission Conf., 1996, vol. 1, no. 423.
- [31] V. I. Utkin, J. Guldner, and J. Shi, Sliding Mode Control in Electromechanical Systems. Boca Raton, FL: CRC, 1999.
- [32] P. Kundur, Power System Stability and Control, N. J. Balu and M. GLauby, Eds. New York: McGraw-Hill, 1994.
- [33] J. J. Grainger and D.W. Stevenson, Power System Analysis, A.B. Akay and E. Castellano, Eds. New York: McGraw-Hill, 1994.
- [34] Narendra Korrapolu, A.Ramanjaneyulu and Dr Y.Rajendra Babu, “Power Flow Enhancement with Better control strategy by DPC and FUZZY logic on UPFC,” *International Journal of Engineering Research-Online* Vol.1, Issue 2, pp. 151–162, 2013.